Phase Behavior and Segmental Mobility in Binary Blends of Polystyrene and Poly(vinyl methyl ether)

Todd Wagler and Peter L. Rinaldi*

Department of Chemistry, The University of Akron, Akron, Ohio 44325-3601

Chang Dae Han* and Hyunaee Chun

Department of Polymer Engineering, The University of Akron, Akron, Ohio 44325-0301

Received June 8, 1999; Revised Manuscript Received November 15, 1999

ABSTRACT: The phase behavior and segmental mobility in binary blends of polystyrene (PS) and poly(vinyl methyl ether) (PVME) were investigated. Two nearly monodisperse PSs having weight-average molecular weights (M_w) of 57 000 and 95 000 with polydispersity indexes (PDI) of 1.06 and 1.09, respectively, and PVME having M_w = 99 000 with a PDI of 2.13 were used for this study. Two sets of PS/PVME binary blends with varying compositions were prepared by solvent casting from toluene. Thermograms from differential scanning calorimetry showed that each blend has a single, yet very broad glass transition temperature. Cloud point measurements via He−Ne laser light scattering were taken to determine phase equilibria in each blend, which exhibited lower critical solution temperature (LCST) behavior. Solid-state nuclear magnetic resonance (NMR) spectroscopy was used to examine segmental mobility and component domain sizes. ^{1}H $T_{1\rho}$ experiments were run at temperatures ranging from −40 to 140 °C. We observed only small differences in ^{1}H $T_{1\rho}$ values of PS and PVME at temperatures below 45−80 °C (depending on blend composition) and a large divergence of ^{1}H $T_{1\rho}$ values at higher temperatures. ^{13}C $T_{1\rho}$ and wide-line separation (WISE) experiments were run at room temperature on untreated and heat-treated samples. WISE experiments revealed that heterogeneities from 3.5 nm to greater than 30 nm existed within the blends, depending on the temperature of heat treatment. Since it has been found that ^{1}H $T_{1\rho}$ measurements can give ambiguous domain information, ^{1}H-NOESY NMR was used to examine several blend compositions at 100 °C. We conclude from this study that nanoheterogeneities exist in these PS/PVME blends at temperatures below the binodal curve determined by cloud point measurements and that a broad, single glass transition should not be construed as evidence of miscibility at the molecular level. It has been shown that nanoheterogeneities exist on a segmental level and that there are large changes in mobility at temperatures above 45−80 °C. However, the blend does not phase separate until the critical temperature (LCST), determined by cloud point measurements, is reached.

Introduction

Often, a polymer blend is regarded as miscible when it exhibits a single glass transition temperature (T_g) and is regarded as immiscible when it exhibits two T_g's corresponding to those of the constituent components as determined by differential scanning calorimetry (DSC) or dynamic mechanical thermal analysis (DMTA). However, there is a general consensus that such experimental techniques, while very useful, cannot guarantee that a polymer blend is miscible on a *molecular level*. DMTA can resolve the size of domains (or separated phases) of the order of 5−10 nm,[1] and DSC is not as sensitive as DMTA to determine the T_g of a polymer blend.[2] Thus, it is fair to state that while DSC and DMTA are useful to investigate macrophase separation in polymer blends, it is not so clear whether a polymer blend can be regarded as being miscible on a molecular level based on DSC or DMTA.

Among the many known miscible polymer blends, those of polystyrene (PS) and poly(vinyl methyl ether) (PVME) have received the most attention. Various aspects of the PS/PVME blends have been investigated, namely, (a) glass transition and/or phase equilibria,[3−13] (b) phase-separated morphology,[5,7,10] (c) the kinetics of phase separation,[14,15] and (d) the dependence of the Flory−Huggins interaction parameter on temperature and blend composition.[16,17] It has also been reported that, among other factors, miscibility windows for the PS/PVME blends depend strongly on the molecular weight of the constituent components.[6,9]

Previous investigators have observed a very broad, single glass transition in such miscible polymer blends, as PS/PVME blends,[10−12] PS/poly(α-methylstyrene) blends,[18−20] and 1,4-polyisoprene/poly(vinylethylene) blends.[21−23] For instance, Schneider and Wirbser[12] have shown that some PS/PVME blends, which exhibit lower critical solution temperature (LCST), undergo a very broad (as broad as 60 °C), single glass transition. Under such circumstances, it is not clear how an unambiguous, single value of T_g can be obtained from a DSC trace. A more serious question can be raised as to whether such a blend can be regarded as being miscible at the segmental level. On the basis of the observations made using electron spin resonance (ESR), Müller et al.[13] reported that certain compositions of poly[styrene-*co*-(maleic anhydride)] (PSMA)/PVME blends have microheterogeneity with domain sizes of approximately 5 nm at temperatures much lower (approximately 70 °C) than its LCST (as determined by cloud point measurement via He−Ne laser light scattering).

As early as 1974, Kwei et al.[4] reported evidence from NMR spectroscopy that PS/PVME blends, which were found to be miscible from a study of *macroscopic* phase behavior, had *microheterogeneity*. Recently, more so-

* Corresponding authors. Peter L. Rinaldi: Telephone 330-972-5990; Fax 330-972-5256; E-mail PeterRinaldi@uakron.edu. Chang Dae Han: Telephone 330-972-6468; E-mail cdhan@uakron.edu.

10.1021/ma9909105 CCC: $19.00
Published on Web 02/12/2000

phisticated NMR techniques, such as cross-polarization magic-angle spinning (CPMAS),[24,25] wide-line separation (WISE),[26] and Goldman−Shen[27] experiments have been used to estimate component domain sizes in polymer blends. Kaplan[28] used some of these techniques in the study of 60/40 and 40/60 PS/PVME blends cast from toluene, where 60/40 and 40/60 refer to the weight percents of the component polymers. He found that the blends were not homogeneous in terms of molecular motion although mixing appeared to have occurred at the segmental level. Schmidt-Rohr et al.[26] used WISE NMR spectroscopy, a modification of the Goldman−Shen experiment,[27] and found that a miscible 50/50 PS/PVME blend contained heterogeneities on the order of 3.5 nm. From the measurements of the proton spin−lattice relaxation in the rotating frame (^{1}H $T_{1\rho}$), Chu et al.[25] investigated the segmental mobility in PS/PVME blends as a function of temperature, blend composition, and molecular weight of PS and concluded that microheterogeneities at a 1 nm scale exist at −5 °C.

Not only can NMR spectroscopy be used to estimate the heterogeneity of a polymer blend, but it can also probe local chain dynamics, which play an important role in understanding the physical properties of these systems. The ^{13}C spin−lattice relaxation in the rotating frame (^{13}C $T_{1\rho}$) and ^{13}C spin−spin relaxation (^{13}C T_2) NMR measurements can be excellent probes to examine individual chain dynamics as a function of temperature in compatible polymer blends.[29,30] These measurements do not suffer from fast spin diffusion, which may obscure the individual relaxation behavior of each component.[30] However, it is proton spin diffusion which will allow us to examine small microdomains, the main interest of this study.

Another interesting observation reported by Bank et al.,[3] who investigated the miscibility of PS/PVME blends via DSC, was that annealing conditions (e.g., the temperature and the duration of annealing and the cooling rate after annealing at an elevated temperature) affected the breadth of the glass transition (and thus the extent of miscibility) of PS/PVME blends. However, to date, the mechanism of such experimental observations has not been explained.

Recently, we investigated (i) glass transitions via DSC under various annealing conditions, (ii) macrophase equilibria via cloud point measurement, and (iii) segmental mobility via solid-state NMR spectroscopy in PS/PVME blends which were cast from toluene. The present study was motivated in part to investigate via NMR spectroscopy whether the presence of microheterogeneity in PS/PVME blends affects the phase diagram determined by cloud point measurements. During DSC analysis, we observed that the cooling rate after the preceding heating cycle greatly affected the glass transition of PS-rich blends in the subsequent heating cycle. However, it had *little* effect on the glass transition of PVME-rich blends. Additionally, NMR studies showed that while nanoheterogeneities exist initially on a segmental level and that there are large changes in mobility at temperatures above 45−80 °C, the blend does not phase separate until the critical temperature (LCST), determined by cloud point measurements, is reached.

Experimental Section

Materials. In this study, we used two anionically polymerized polystyrenes, one having a weight-average molecular weight (M_w) of 57 000 and a polydispersity index (PDI) of 1.06 (hereafter referred to as PS57) and another having M_w = 95 000 and a PDI of 1.09 (hereafter referred to as PS95). Each of the two polystyrenes was blended, via solution casting from toluene, with PVME (Scientific Polymer Products) having M_w = 99 000 (hereafter referred to as PVME99) and a PDI of 2.13. The molecular weights and molecular weight distributions of the PSs were determined via gel permeation chromatography. Calibration curves for PS were constructed using 10 monodisperse PS standards (Scientific Polymer Products) having M_w ranging from 2×10^3 to 2×10^6.

Sample Preparation. Blends with various compositions were prepared by solution casting from toluene. Predetermined amounts of the polymer(s) were dissolved in toluene to make 5 wt % solutions, in which 0.1 wt % of an antioxidant (Irganox 1010, Ciba-Geigy Group) was added to prevent thermal decomposition of the samples. The solvent was evaporated slowly at room temperature for 1 week. The samples were then put into a vacuum oven at 40 °C first without vacuum, and then the vacuum was applied very slowly in order to prevent the formation of bubbles during the evaporation of the solvent. This step of drying continued for about 2 weeks. The sample was dried further by applying full vacuum at 40 °C for about 1 month. The oven temperature was then raised to 60 °C first without vacuum, and then the vacuum was applied very slowly in order to prevent bubble formation during the evaporation of the solvent. This step of drying continued for about 1 week. Finally, full vacuum was applied to the samples at 60 °C, and the drying was continued for 2 days. For PS-rich samples (neat PS, 80/20, 70/30, and 60/40 PS/PVME blends), we adopted the following additional procedures to further dry the samples. For the 60/40 PS/PVME blend, the oven temperature was raised to 70 °C first without vacuum, then the vacuum was applied very slowly over about 1 h, and then full vacuum was applied for 1 day. For the 70/30 PS/PVME blend, the oven temperature was raised to 80 °C first without vacuum, then the vacuum was slowly applied to the sample over 2−3 h, and then full vacuum was applied for 1 day. For the 80/20 PS/PVME blend, the oven temperature was first raised to 90 °C without vacuum, then the vacuum was applied to the sample very slowly over 2−3 h, and then full vacuum was applied for 1 day. For neat PS, the oven temperature was raised to 100 °C first without vacuum, then the vacuum was slowly applied over 2−3 h, and then full vacuum was applied for 1 day. All blend samples were put into a vacuum oven at 100 °C first under a partial vacuum, and then the vacuum was applied very slowly to remove any residual solvent in the samples. The drying was continued until there was no bubble formation in each sample. All samples were checked for bubble formation at the end of preparation using optical microscopy.

Differential Scanning Calorimetry (DSC). The glass transition temperature (T_g) of each blend was measured using DSC (Perkin-Elmer DSC 7 series). Prior to measurement, the baseline was established using two empty pans. To prevent thermal degradation, nitrogen gas was circulated around the sample pan. Each sample of about 15 mg was first heated to 120 °C at a heating rate of 10 °C/min, annealed there for 3 min, and then quenched to room temperature at a cooling rate of 200 °C/min. The second heating was used to determine the T_g of the specimen. As will be shown below, PS/PVME blends at certain compositions exhibit very broad glass transitions. Therefore, the following notations will be used: (a) T_{gi} for an onset point of glass transition, (b) T_{gm} for the midpoint of glass transition, and (c) T_{gf} for the final point of glass transition.

Cloud Point Measurement. Cloud points for PS/PVME blends were determined using a He−Ne laser light scattering instrument with a heating rate of 1 °C/min. The detection angle of 20° was chosen.

Solid-State NMR Spectroscopy. Solid-state NMR spectra were obtained using a Varian Unityplus-200 (4.7 T) spectrometer with a Doty Scientific standard variable temperature magic angle spinning (VTMAS) probe and a Doty Scientific supersonic VTMAS probe. The polymer films were packed into 7 mm silicon nitride rotors with macor O-ring end caps for extended temperature studies or 7 mm silicon nitride rotors

with Kel-F end caps for high MAS rates. Spectra were acquired at spinning speeds ranging from 2 to 6 kHz. All ^{13}C and ^{1}H chemical shifts were corrected by using hexamethylbenzene ($\delta_{Me} = 17.3$ ppm) or deuterated chloroform ($\delta_{CDCl_3} = 7.24$ ppm) as an external reference, respectively. Temperature calibration was performed using lead nitrate[31] and yielded temperatures that were accurate to within ±2 °C. Temperature control was maintained by a Doty Scientific VT controller. The following experiments were performed:

***$T_{1\rho}$* Measurements.** ^{1}H $T_{1\rho}$'s were measured indirectly by using the standard CPMAS technique,[24] with the addition of a variable spin-lock time inserted between the initial 90° pulse and the cross-polarization time. The ^{1}H spin-lock time was varied from 0 to 40 ms with a lock field $\gamma B_1 = 55$ kHz. The cross-polarization time was held constant during each experiment. However, the time chosen varied with temperature in order to capture the greatest distribution of spins (400 μs to 2 ms). A decoupling field strength of 60 kHz was used in all experiments. Experiments were carried out at temperatures ranging from −40 to 140 °C. Every attempt was made to run each sample continuously throughout the temperature range to avoid different thermal histories for the samples. Each ^{1}H $T_{1\rho}$ measurement required 4−12 h of experiment time.

WISE-2D Experiments. ^{1}H wide-line spectra were acquired with the use of the WISE-2D NMR pulse sequence developed by Schmidt-Rohr et al.[26] The pulse sequence consists of a $90°_{X}$ pulse, which flips the magnetization into the *xy* plane, followed by a t_1 evolution period. Next a $90°_{-X}$ pulse is applied to flip the magnetization back to the *z*-axis. The magnetization was then allowed to diffuse during a constant mixing period (t_m), which ranged from 100 μs to 40 ms. After the mixing period another $90°_{X}$ pulse flips the ^{1}H magnetization back into the transverse plane where it is immediately subjected to cross-polarization from protons to carbons. The acquisition period (t_2) consists of the modulated ^{13}C signals. The experiment reveals proton wide-line spectra from the protons of PS and PVME along the ω_1 dimension, resolved by the ^{13}C chemical shifts of PS and PVME along the ω_2 dimension. A correlation can then be made between the chemical structure and segmental mobility of the blend.

This experiment was used to analyze fresh samples of the 20/80, 30/70, 50/50, 70/30, and 80/20 PS95/PVME99 blends at room temperature. It was also used to study samples of the 30/70, 50/50, and 70/30 blends that were thermally heat-treated at various temperatures. Heat treatment was carried out in a vacuum oven at temperatures ranging from 80 to 140 °C. The majority of sample treatments lasted for 12 h at the specified temperature. However, samples of the 70/30 PS/PVME blend were subjected to additional heat treatments in an attempt to understand the effects of prolonged heat treatment and heating rates. Specifically one sample was treated at 100 °C for 1 week. A second sample was created from seven individual 15 mg samples. Each of these 15 mg samples was first cooled to −30 °C and then heated to 90 °C at a heating rate of 10 °C/min. They were then quenched rapidly from 90 to −40 °C at a rate of 200 °C/min and heated to 100 °C at a rate of 10 °C/min. These heat treatments were performed in the DSC-7 instrument and were a replication of DSC measurements. The following applied for all blend samples; at the end of each heat treatment the sample was quenched in liquid nitrogen and the experiment run at room temperature. Spectral windows of 20 and 200 kHz were used for the ω_2 and ω_1 dimensions, respectively. Between 32 and 128 t_1 increments were used in the 2D experiments. The cross-polarization and the decoupling field strengths were the same as those used for the ^{1}H $T_{1\rho}$ experiments.

***^{13}C $T_{1\rho}$* Experiments.** ^{13}C $T_{1\rho}$ data can be obtained by using the standard cross-polarization experiment with the addition of a ^{13}C spin-lock pulse inserted between the acquisition and cross-polarization periods. The ^{13}C $T_{1\rho}$ experiment was used in conjunction with the WISE experiment to examine segmental mobility of the heat-treated samples. Therefore, all the samples listed above for the WISE experiments were also studied using this technique. Experiments were run at room temperature.

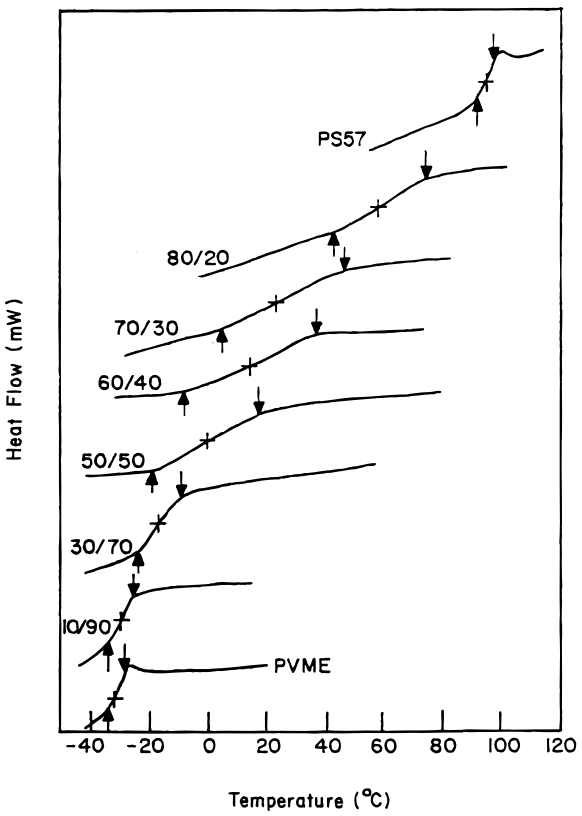

Figure 1. DSC traces for PS57/PVME99 blends, where the arrow pointing upward denotes the temperature (T_{gi}) at which the transition begins, the arrow pointing downward denotes the temperature (T_{gf}) at which the transition ends, and the cross (+) denotes the midpoint (T_{gm}) of the transition. The heating rate employed was 10 °C/min.

^{1}H 2D-NOESY Experiments. ^{1}H NOESY NMR experiments were run at 100 °C on the 70/30, 50/50, and 30/70 PS/PVME blend samples. The experiment used was a standard solution state ^{1}H 2D-NOESY experiment and did not contain any multipulse line narrowing techniques. All experiments were run at 100 °C at a MAS rate of 2.5 kHz to achieve adequate resolution. Bloch decay experiments were performed in conjunction with the NOESY experiments in order to compare spin populations.

Results

Glass Transition Behavior of PS/PVME Blends. Figure 1 shows DSC traces for PS57/PVME99 blends, and Figure 2 shows DSC traces for PS95/PVME99 blends, where the upward arrow denotes the onset point (T_{gi}), the cross (+) denotes the midpoint (T_{gm}), and the downward arrow denotes the final point (T_{gf}) of the glass transition. Table 1 shows a summary of the glass transition temperatures of the blends. It can be seen in Figures 1 and 2 that a single glass transition temperature is observed for each blend composition and that the glass transition becomes very broad for blends containing 0.5−0.8 weight fraction of PS. Furthermore, the glass transition behavior given in Figures 1 and 2 is slightly sensitive to the molecular weight of the PS employed. However, we found in the present study that the breadth of the glass transition for PS-rich blends was very much dependent upon the cooling rate employed after the preceding heating cycle. We elaborate on this below.

Figure 3 shows DSC traces for a 30/70 PS57/PVME99 blend treated under two different annealing conditions. Curve 1 was obtained during heating from −40 to 30

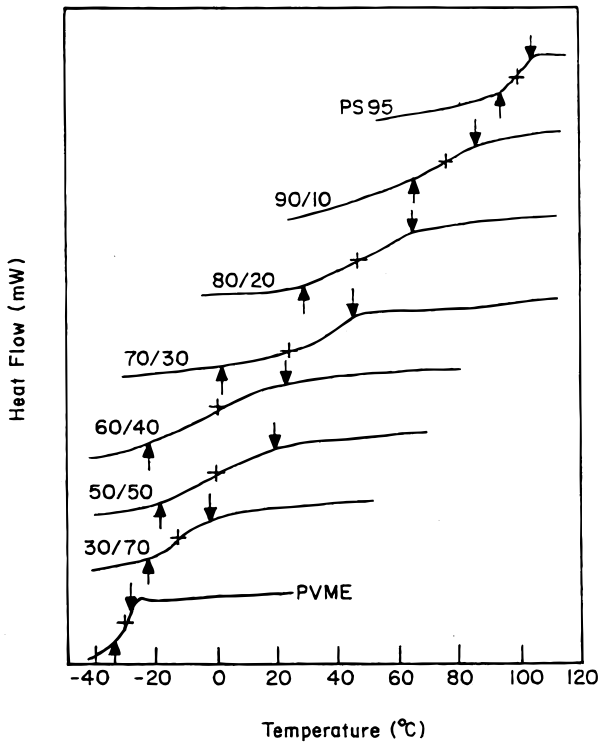

Figure 2. DSC traces for PS95/PVME99 blends, where the arrow pointing upward denotes the temperature (T_{gi}) at which the transition begins, the arrow pointing downward denotes the temperature (T_{gf}) at which the transition ends, and the cross (+) denotes the midpoint (T_{gm}) of the transition. The heating rate employed was 10 °C/min.

Table 1. Glass Transition Temperatures for the PS/PVME Blends Investigated

sample code	T_{gi} (°C)	T_{gm} (°C)	T_{gf} (°C)	$T_{gf} - T_{gi}$ (°C)
(a) PS57/PVME99 Blends				
PS57	92	94	97	5
90/10 PS57/PVME99	66	79	92	26
80/20 PS57/PVME99	43	58	73	30
70/30 PS57/PVME99	5	26	47	42
60/40 PS57/PVME99	−10	13	36	46
50/50 PS57/PVME99	−19	−1	16	35
30/70 PS57/PVME99	−23	−18	−12	11
10/90 PS57/PVME99	−33	−29	−26	7
PVME99	−33	−30	−28	5
(b) PS95/PVME99Blends				
PS95	94	99	104	10
90/10 PS95/PVME99	62	73	84	22
80/20 PS95/PVME99	28	45	62	34
70/30 PS95/PVME99	0	93	46	46
60/40 PS95/PVME99	−23	0	22	45
50/50 PS95/PVME99	−19	1	17	36
30/70 PS95/PVME99	−23	13	−4	19
PVME99	−33	−30	−28	5

°C at a rate of 10 °C/min after the specimen was cooled from 110 to −40 °C at a rate of 10 °C/h (*slow cooling*). Curve 2 was obtained during heating from −40 to 30 °C at a rate of 10 °C/min after the specimen was cooled from 30 to −40 °C at a rate of 200 °C/min (*fast cooling*). It can be seen from Figure 3 that the cooling rate applied to a specimen at the end of the preceding heating cycle had *little* influence on the glass transition in the subsequent heating cycle.

On the other hand, we observe a significant effect of cooling rate on the glass transition of PS-rich blends. Specifically, let us examine DSC traces for a 70/30 PS95/PVME99 blend, shown in Figure 4, which were obtained

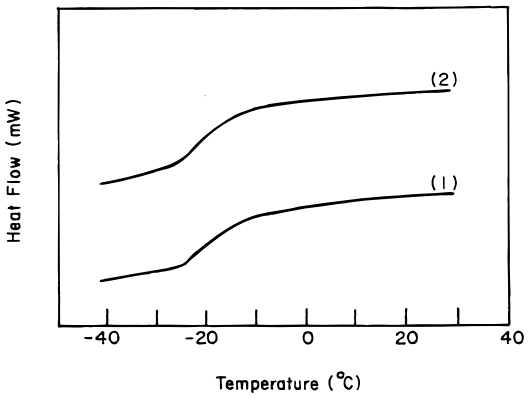

Figure 3. DSC traces for a 30/70 PS57/PVME99 blend, where curve 1 was obtained while heating from −40 to 30 °C at a rate of 10 °C/min after a specimen had been cooled from 110 to −40 °C at a rate of 10 °C/h (slow cooling) and curve 2 was obtained during heating from −40 to 30 °C at a rate of 10 °C/min after a specimen had been cooled from 30 to −40 °C at a rate of 200 °C/min (fast cooling).

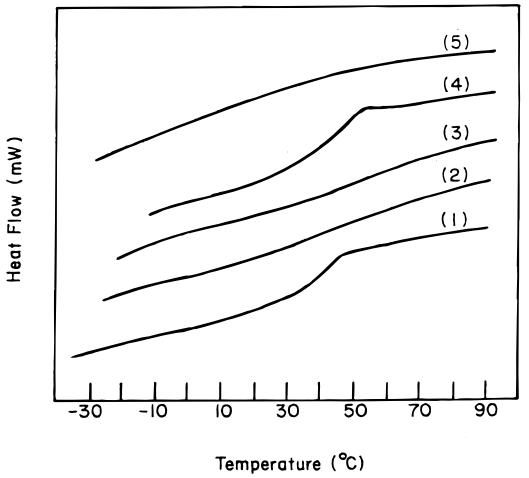

Figure 4. DSC traces for a 70/30 PS95/PVME99 blend. Curve 1 was obtained while heating a fresh specimen from −30 to 90 °C at a rate of 10 °C/min (the first heating cycle); curve 2 was obtained during the second heating cycle from −40 to 100 °C at a rate of 10 °C/min after the specimen was quenched from 90 to −40 °C at a rate of 200 °C/min (*fast cooling*); curve 3 was obtained during the third heating cycle from −40 to 110 °C at a rate of 10 °C/min after the specimen was quenched from 100 to −40 °C at a rate of 200 °C/min (*fast cooling*); curve 4 was obtained during the fourth heating cycle from room temperature to 120 °C at a rate of 10 °C/min after the specimen was annealed at 110 °C for 24 h and then cooled very slowly to room temperature at a rate of 10 °C/h (*slow cooling*); curve 5 was obtained during the fifth heating cycle from −40 to 120 °C at a rate of 10 °C/min after the specimen was cooled from 120 to −40 °C at a rate of 10 °C/min.

at various cooling rates. Curve 1 was obtained while heating a fresh specimen from −30 to 90 °C at a rate of 10 °C/min (the first heating cycle). It can be seen that curve 1 exhibits a broad, yet distinct, single glass transition (T_{gi} = 0 °C, T_{gm} = 23 °C, T_{gf} = 46 °C). After completion of the first heating cycle, the specimen was quenched rapidly from 90 to −40 °C at a rate of 200 °C/min (*fast cooling*) and then subjected to a second heating cycle to 100 °C at a rate of 10 °C/min. Curve 2 was obtained during the second heating cycle at a rate of 10 °C/min. In curve 2 the breadth of the glass transition has increased so much that it is very difficult to unambiguously determine the glass transition temperature of the specimen. After completion of the second

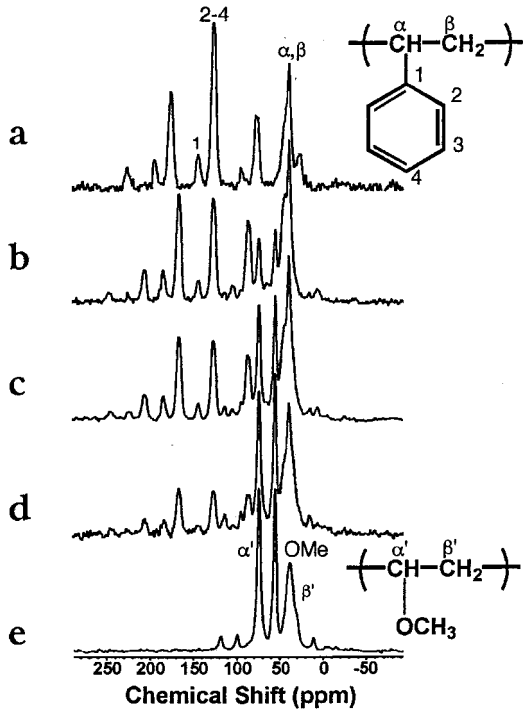

Figure 5. ^{13}C CPMAS spectra at −40 °C of (a) PS95, (b) a 70/30 PS95/PVME99 blend, (c) a 50/50 PS95/PVME99 blend, (d) a 30/70 PS95/PVME99 blend, and (e) PVME99.

heating cycle, the specimen was rapidly quenched from 100 to −40 °C at a rate of 200 °C/min (*fast cooling*) and then subjected to a third heating cycle to 110 °C at a rate of 10 °C/min. Curve 3 in Figure 4 shows the DSC trace for the third heating cycle, which has a shape almost identical to that of curve 2. After completion of the third heating cycle, the specimen was removed from the DSC unit, annealed in a vacuum oven at 110 °C for 24 h, and then cooled very slowly at a rate of 10 °C/h to room temperature (*slow cooling*). When this specimen was subjected to a fourth heating cycle to 120 °C at a rate of 10 °C/min, we obtained curve 4, the shape of which is *virtually* identical to that of curve 1; i.e., we were able to reproduce the glass transition behavior of the fresh specimen. After completion of the fourth heating cycle, the specimen was cooled from 120 to −40 °C at a rate of 10 °C/min and then subjected to a fifth heating cycle. Curve 5 was obtained during the fifth heating cycle from −40 to 120 °C at a rate of 10 °C/min. The shape of this curve is very similar to those of curves 2 and 3. The above observations lead us to conclude that, for a PS-rich 70/30 PS95/PVME99 blend, the cooling rate after the preceding heating cycle played a decisive role in determining the shape, and thus the breadth, of the glass transition in the subsequent heating cycle.

^{13}C NMR Spectra of PS/PVME Blends. The ^{13}C cross-polarization magic angle spinning (CPMAS) spectra at −40 °C of PS, PVME, and various PS/PVME blends used in this study are shown in Figure 5. The labels on the spectra refer to the carbon resonance assignments of the six peaks in the spectra to the atoms shown in the structures. The remaining peaks in the ^{13}C NMR spectra are due to spinning sidebands from both PS and PVME. When the MAS rate is smaller than the chemical shift anisotropy, the spectrum will show sidebands separated by the spinning frequency symmetrically placed about the peak at the isotropic chemical shift.[32] Confirmation of spinning sidebands was made by running the experiment at a different MAS rate. At −40 °C, PVME becomes rather rigid, and its chemical shift anisotropy is large. Overlapping peaks with sidebands were avoided as much as possible. At temperatures above −20 °C, spinning sidebands from PVME are no longer noticeable.

Measurements of ^1H $T_{1\rho}$. The ^1H $T_{1\rho}$ experiment reveals not only the proton spin−lattice relaxation rate in the rotating frame but also the primary repeat unit structure. Even in the PS/PVME blends, it is possible to resolve a distinct carbon resonance from each of the blend's components. Additional information can be gained from these experiments since ^1H $T_{1\rho}$'s are susceptible to segmental motions at the spin-lock field strength. A minimum in ^1H $T_{1\rho}$ is observed when the greatest distribution of segmental motions has a frequency of 55 kHz. In the present study, the oxymethine ($\delta = 76$ ppm) of PVME and the phenyl group ($\delta = 126$ ppm) of PS were chosen for comparison because they were well resolved, and spin diffusion was most effective between these sites over the temperature range studied. It has generally been accepted that if the component polymers in a blend exhibit a common ^1H $T_{1\rho}$, then the blend is homogeneous on a scale of a few nanometers.[33] However, as will be shown below, if the spin diffusion rate is rather slow, even a completely amorphous homopolymer can give different ^1H $T_{1\rho}$ values for the different functional groups on the polymer. The rate of spin diffusion must be considered when evaluating ^1H $T_{1\rho}$ data.

^1H $T_{1\rho}$'s were measured from the decay of magnetization during the ^1H spin-lock pulse, before cross-polarization. In most cases a single-exponential fit was adequate for describing the relaxation behavior. However, in some cases, the fits were clearly best described by a biexponential function. In those cases, the long component was used when plotting ^1H $T_{1\rho}$ values versus temperature. It should be noted that biexponential behavior is a sign of phase separation, where PS-rich and PVME-rich domains might coexist.[25] However, biexponential behavior may have been obscured at high temperatures when long cross-polarization times were used, eliminating the short component.

Homopolymer PS. Figure 6 shows plots of ^1H $T_{1\rho}$ versus temperature for the aromatic and backbone protons of pure PS. In Figure 6 we observe that ^1H $T_{1\rho}$ values decrease monotonically with temperature, approaching a minimum at 120 °C, consistent with the high T_g (100 °C) and rigidity of this polymer. It is evident that the ^1H $T_{1\rho}$ values of PS decrease as the glass transition region is approached. Menestrel et al.[34] found from ^{13}C line width measurements that the aromatic and main chain carbons are involved in correlated motions. ^1H $T_{1\rho}$ values are essentially equal for the phenyl ring and backbone protons throughout the temperature range studied. Spin diffusion is very effective in equilibrating the magnetization and relaxation behavior. At the ^1H $T_{1\rho}$ minimum, there is a substantial amount of molecular motion at the spin-lock frequency (55 kHz).

Homopolymer PVME. As can be seen in Figure 7, pure PVME has very different motional characteristics when compared to pure PS. First, pure PVME shows a minimum in ^1H $T_{1\rho}$ just above 0 °C, consistent with its pliability and low T_g (−25 °C). Second, the methoxy group ($\delta = 56$ ppm) contains an extra degree of motional

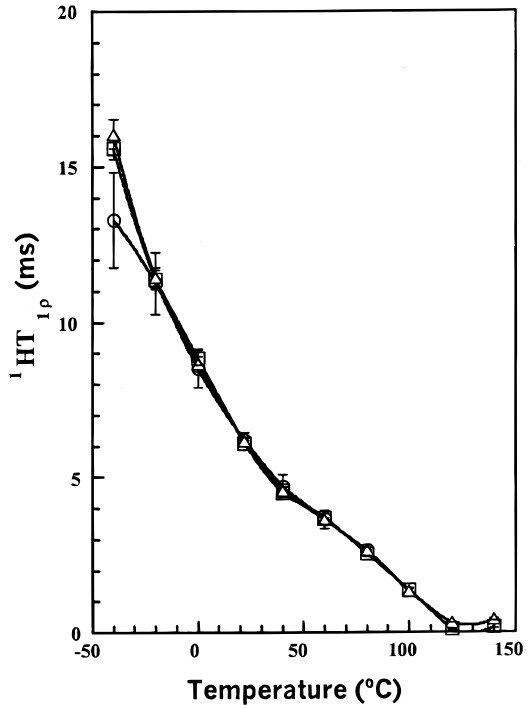

Figure 6. Plots of ^1H $T_{1\rho}$ versus temperature for homopolymer PS95: (○) nonprotonated aromatic carbon at $\delta = 146$ ppm; (△) protonated aromatic carbons at $\delta = 126$ ppm; (□) methylene and methine carbons at $\delta = 40$ ppm.

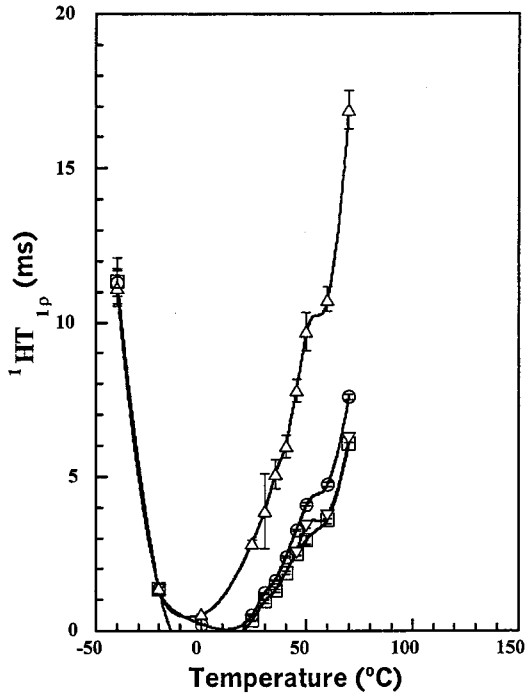

Figure 7. Plots of ^1H $T_{1\rho}$ versus temperature for homopolymer PVME99: (○) oxymethine carbon at $\delta = 76$ ppm; (△) methoxy carbon at $\delta = 56$ ppm; (□) methylene (meso) carbon at $\delta = 40$ ppm; (▽) methylene (racemic) carbon at $\delta = 39$ ppm.

freedom which allows it to move more freely than the main chain. As the temperature is increased above 0 °C, the frequency of the molecular motion increases, resulting in longer ^1H $T_{1\rho}$'s. Rapid motion of the methoxy group results in slow spin diffusion between the methoxy methyl and backbone protons. Asano et al.[35] found that at 38 °C the spin diffusion rate between OCH_3 and the main chain of PVME was 100 s^{-1},

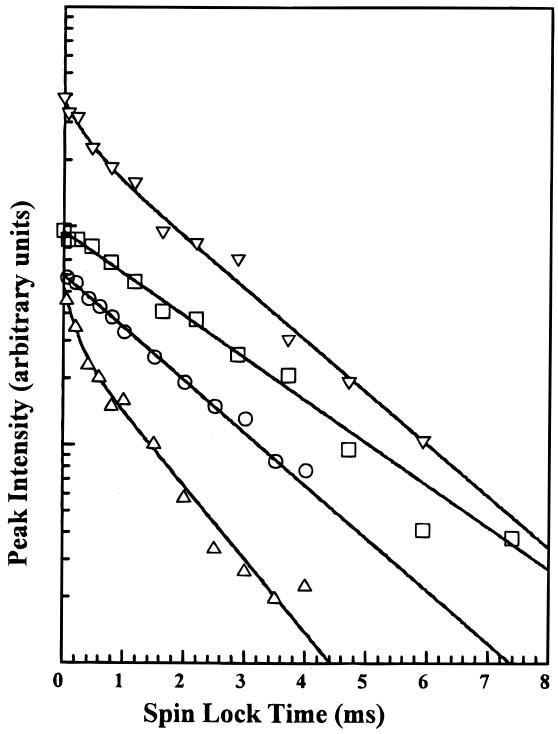

Figure 8. Plots of peak intensity versus spin-lock time (decay curves) for (○) 20/80 PS95/PVME99 blend at $\delta = 126$ ppm, (△) 20/80 PS95/PVME99 blend at $\delta = 76$ ppm, (□) 30/70 PS95/PVME99 blend at $\delta = 126$ ppm, and (▽) 30/70 PS95/PVME99 blend at $\delta = 76$ ppm.

whereas the spin diffusion rate between PS and the main chain of PVME is 1.1×10^3 s^{-1}. While multicomponent relaxation behavior was observed at temperatures between 30 and 50 °C for the methoxy group, the oxymethine group exhibited only single-component relaxation behavior over the entire temperature range studied for the PVME homopolymer. Rapid motion and slow spin diffusion of the methoxy group to the rest of the system were observed in all of the blends studied. From a plot of ln(^1H $T_{1\rho}$) versus temperature (not shown here) we observe that the rate of increase in ^1H $T_{1\rho}$ is essentially equal for the backbone and methoxy group of PVME. At temperatures above 45 °C, the PVME methylene carbons in the meso ($\delta = 40$ ppm) and racemic ($\delta = 39$ ppm) diads are resolved.

PS/PVME Blends. Multicomponent relaxation behavior was observed in our PS/PVME blends, similar to the study of Chu et al.[25] They found that PS100/PVME74 blends with less than 50 wt % PS content exhibited biexponential behavior at −5 °C. This suggests that the blends are microheterogeneous on a 1 nm scale. Figure 8 shows plots of spin-lock time versus peak intensity for the 20/80 and 30/70 PS95/PVME99 blends at 0 °C. While the oxymethine group in pure PVME shows only a single-exponential decay at 0 °C, it can clearly be seen that the oxymethine relaxation is biexponential for blends with high PVME content. Multicomponent relaxation was observed at least once over the temperature range studied for all of the blends used in this study.[36] Unfortunately, there was no significant trend in the data where single-component decays evolved into multicomponent decays as the temperature was increased. The lack of any significant trend may stem from the fact that the initial magnetization decay may have been obscured in the ^1H $T_{1\rho}$ experiment conducted in this study. Also, a low signal-to-noise ratio might

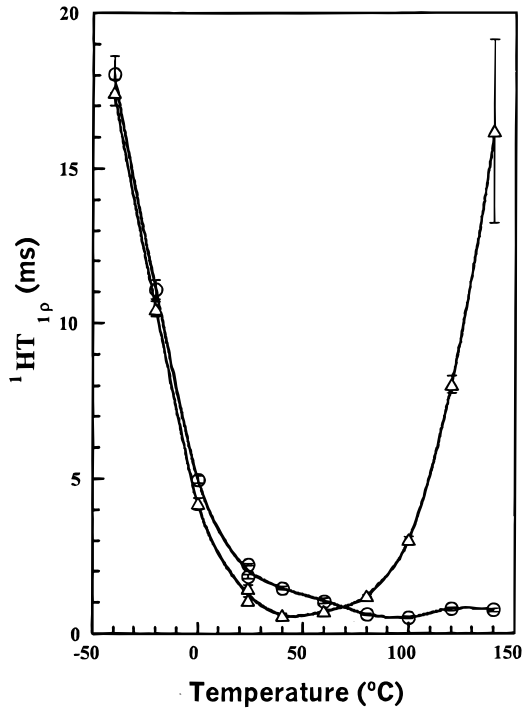

Figure 9. Plots of ^1H $T_{1\rho}$ versus temperature for a 50/50 PS95/PVME99 blend: (○) protonated aromatic carbons at $\delta = 126$ ppm; (△) oxymethine carbon at $\delta = 76$ ppm.

have resulted in detection of only single-exponential decays if the fraction of the fast component was low.

While multicomponent ^1H $T_{1\rho}$ relaxation can signify microphase separation, additional information was found by monitoring ^1H $T_{1\rho}$ as a function of temperature. Figure 9 shows a plot of ^1H $T_{1\rho}$ versus temperature for a 50/50 PS95/PVME99 blend. The ^1H $T_{1\rho}$'s for the protonated aromatic ($\delta = 126$ ppm) and oxymethine ($\delta = 76$ ppm) carbons exhibit parallel behavior from −40 to 80 °C. Although small differences in ^1H $T_{1\rho}$ do exist, cooperative motion is still observed. These small differences in ^1H $T_{1\rho}$'s indicate that the blend is not completely homogeneous, even at room temperature. Others[25,26,28] have already reported that PS/PVME blends are heterogeneous on the segmental level and contain small initial domains on the order of 0.6−3.5 nm at temperatures where other methods (e.g., light scattering) indicate the blends to be homogeneous. At temperatures above 80 °C, the frequency of molecular motion in PVME increases dramatically while molecular motion in PS remains approximately constant with a large distribution of motions at 55 kHz. This blend exhibited the broadest minimum in ^1H $T_{1\rho}$. Similar observations were made for the 60/40 and 70/30 PS95/PVME99 blends, except that the rate of increase of ^1H $T_{1\rho}$ values after 80 °C was greater for PVME. Menestrel et al.[34] found that as the proportion of PS in PS/PVME blends becomes greater, the local motions of the PVME chains increase when the temperature reaches the glass transition of the blend. In addition, they found that the fractional free volume for the PVME units at the glass transition of the blend increased with increasing PS content in the blend. The increase in free volume may allow the PVME component in the blend to behave more like the homopolymer PVME.

Plots of ^1H $T_{1\rho}$ versus temperature for the 20/80 and 30/70 PS95/PVME99 blends were also constructed, not shown here. As the amount of PS decreased, so did the

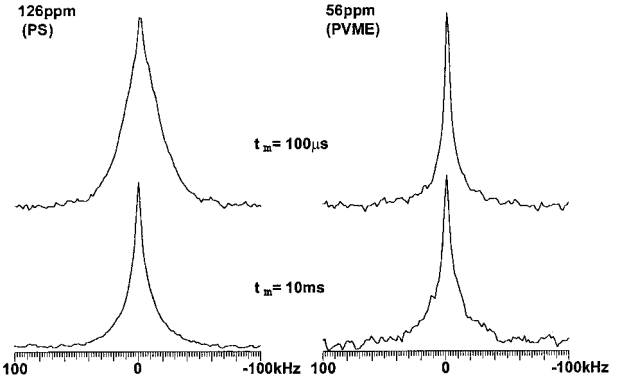

Figure 10. Series of proton wide-line spectra for a fresh 50/50 PS/PVME blend. At 100 μs the ^1H line widths of PS (27.5 kHz) and PVME (6.5 kHz) are significantly different, representing rigid and mobile domains for PS and PVME, respectively. At 10 ms the ^1H line widths of PS (10.7 kHz) and PVME (9.3 kHz) are equivalent.

temperature required to create a divergence in ^1H $T_{1\rho}$ values. The ^1H $T_{1\rho}$'s for the protonated aromatic ($\delta = 126$ ppm) and oxymethine ($\delta = 76$ ppm) carbons exhibited parallel behavior from −40 to 45 °C, and then a large divergence occurred. For the 20/80 PS95/PVME99 blend, at temperatures above 20 °C, the frequency of molecular motion in PVME increased dramatically while molecular motion in PS increased only slightly and then leveled off as the temperature was raised above 50 °C. Similar results were observed in the 30/70 PS95/PVME99 blend.

2D-WISE Measurements. WISE NMR can be used to determine the mobilities of PS and PVME separately and to characterize the phase composition of the blend on a scale of 1−30 nm.[26,37] The experiment shows proton wide-line spectra from the protons of PS and PVME along the ω_1 dimension, resolved by the ^{13}C chemical shifts of PS and PVME along the ω_2 dimension. Figure 10 shows a series of ^1H wide-line slices along the ω_1 dimension for a fresh untreated 50/50 PS95/PVME99 blend with mixing times of 100 μs and 10 ms. Slices were taken from the most intense ^{13}C resonances of the protonated aromatic carbons (PS $\delta = 126$ ppm) and of the methoxy carbon (PVME $\delta = 56$ ppm). At a mixing time of 100 μs, PVME shows a narrow proton line width (6.5 kHz) corresponding to high mobility while PS shows a rather broad line width (27.5 kHz) which indicates more rigid segments. However, at a mixing time of 10 ms there is a substantial decrease in the aromatic proton line widths while the methoxy proton line width has increased by only 3 kHz. Proton spin diffusion during the mixing time has resulted in the ^{13}C signals being modulated by the same ^1H decay. Therefore, the ^{13}C modulated signals exhibit essentially the same ^1H line shape for the aromatic (10.7 kHz) and methoxy (9.3 kHz) protons. Experimental error for determination of the ^1H line widths from the WISE experiments was found to be ±2.2 kHz. These experiments revealed that the ^1H line widths for untreated samples of the 20/80, 30/70, 50/50, 70/30, and 80/20 PS95/PVME99 blends had equilibrated between 5 and 10 ms. Schmidt-Rohr et al.[26] found that the smallest diameter of a typical heterogeneity in a 50/50 PS200/PVME50 blend system at 320 K was 3.5 ± 1.5 nm, where the ^1H line widths equilibrated after 5 ms. Using the equation and diffusion coefficient[38] from their paper,[26] we have found similar results for our untreated samples of the 20/80, 30/70, 50/50, 70/30, and 80/20 PS95/PVME99 blends at room tempera-

Table 2. WISE Line Width Results for Heat-Treated 30/70 PS/PVME Blends

	fwhh[a] (kHz) at mixing time (ms) of					
	1	5	10	50	100	200
untreated/126 ppm	17.8	12.1	10.7			
untreated/56 ppm	9.3	9.5	9.3			
heat treatment/peak						
120 °C for 12 h/126 ppm	17.2	11.9	11.4			
120 °C for 12 h/56 ppm	10.3	10.9	10.6			
140 °C for 12 h/126 ppm	31.7	28.8	29.1	27.5	26.8	24.9
140 °C for 12 h/56 ppm	7.2	7.4	7.5	7.7	7.5	7.5

[a] Measured line widths at peak half-height.

Table 3. WISE Line Width Results for Heat-Treated 50/50 PS/PVME Blends

	fwhh[a] (kHz) at mixing time (ms) of					
	1	5	10	50	100	200
untreated/126 ppm	16.7	12.0	10.7			
untreated/56 ppm	7.8	9.1	9.2			
heat treatment/peak						
80 °C for 12 h/126 ppm	17.8	13.2	11.6			
80 °C for 12 h/56 ppm	11.0	11.4	10.2			
100 °C for 12 h/126 ppm	18.6	14.4	13.8			
100 °C for 12 h/56 ppm	11.5	13.5	12.7			
120 °C for 12 h/126 ppm	17.8	13.8	12.0			
120 °C for 12 h/56 ppm	10.1	10.4	10.5			
140 °C for 12 h/126 ppm	24.6	23.2	22.5	22	19.6	20.5
140 °C for 12 h/56 ppm	6.3	6.7	7.9	7.2	8.0	7.8
140 °C for 12 h followed by annealing at 100 °C for 24 h/126 ppm	18.9	14.7	13.4			
140 °C for 12 h followed by annealing at 100 °C for 24 h/56 ppm	9.6	10.1	12.6			

[a] Measured line width at peak half-height.

ture. Calculation of the domain size revealed that the difference between an equilibrating mixing time of 5 and 10 ms was 3.5 ± 1.5 and 4.9 ± 1.7 nm, respectively.

Further studies were conducted on portions of the 30/70, 50/50, and 70/30 PS95/PVME99 blend samples that were heat treated at various temperatures. Experiments were carried out at room temperature, because at high temperatures where the T_2's of PS and PVME differ by a factor of 4, calculation of an accurate diffusion coefficient is highly suspect. Table 2 shows the WISE ^{1}H line width results for portions of the 30/70 blend that were untreated, treated for 12 h at 120 °C, and treated for 12 h at 140 °C. From the table it can clearly be seen that the ^{1}H line widths for the untreated sample and the sample that was treated at 120 °C behave essentially the same. The ^{1}H line widths of the protonated aromatic carbons (126 ppm) and the methoxy carbons (56 ppm) equilibrate after a mixing time of 10 ms. However, the sample that was treated at 140 °C never achieves proton line width equilibration even after 200 ms. Nonequilibration of the ^{1}H line widths demonstrates that domains larger than 30 nm exist within the blend.[26]

Table 3 shows the WISE ^{1}H line width results for portions of the 50/50 PS95/PVME99 blend sample that were treated at 80, 100, 120, and 140 °C for 12 h. The data reveal that all treated samples share similar ^{1}H line width behavior except for the sample that was treated at 140 °C for 12 h. This sample never achieves proton line width equilibration even after 200 ms. This temperature is above the LCST as determined by light scattering. The final two rows of Table 3 contain results from additional treatment of the 50/50 blend that was treated at 140 °C for 12 h. This sample was also used in a 2D-NOESY experiment that was run at 100 °C. After this experiment was completed, it was observed that the sample turned from completely opaque (white) to clear, indicating macroscopic homogeneity. In addition, the NOESY results suggested that the blend was homogeneous on a segmental level. The WISE experiment was then run at room temperature and revealed something very interesting. It showed that the proton line widths for PS and PVME equilibrate after a mixing time of 10 ms. Davis et al.[7] showed that an immiscible blend of PS/PVME made from trichloroethylene could become miscible again if the sample was annealed at temperatures ranging from 60 to 100 °C, depending on blend composition. Moreover, our results correlate well with the results of Nishi et al.,[5] who showed that by cycling the temperature just above and below the cloud point that they could transform the blend from clear to opaque to clear again. However, here we have the added bonus that we can determine, without relying on low resolution optical methods, that the blend is homogeneous on a scale of 5 nm.

Table 4 shows line widths for an untreated 70/30 blend as well as portions of the 70/30 PS95/PVME99 blend that were treated at 100, 120, and 140 °C. The sample treated at 100 °C was treated for 1 week to ascertain whether prolonged heating would induce phase separation. Also reported are line widths from the 70/30 PS95/PVME99 blend sample composed of seven individual 15 mg samples that were subjected to DSC heating rates in accordance with curves 1 and 2 in Figure 4. As can be seen from Table 4, prolonged heating at 100 °C for 1 week does not induce phase separation. In addition, even though the glass transition of the blend broadens severely to the point where it was indiscernible in curve 2 of Figure 4, the WISE experiment revealed that there was no change in domain size. Only after the sample was treated at 140 °C did the line widths cease to equilibrate at 10 ms. The results in Table 4 shows that the line widths are larger overall than the corresponding line widths for both the 30/70 and 50/50 PS95/PVME99 blends. The main reason for the increase in line width results from an overall increase in the rigidity of the blend.

^{13}C $T_{1\rho}$ Measurements. ^{13}C $T_{1\rho}$ measurements were run in conjunction with the WISE experiment to understand the effect of heat treatment on segmental motion. In all cases there were multicomponent decays, where biexponential fits described the decays adequately. The percentage of the slow relaxing component is reported for the protonated aromatic carbons ($\delta = 126$ ppm) of PS. The errors associated with the calculation of the fraction of slow relaxing component for PS was below 5% in all cases. Unfortunately, the error was extremely high (up to 50%) when calculating the fraction of the slow relaxing component for the oxymethine carbons ($\delta = 76$ ppm) of PVME. These large errors probably result from the fact that the peak intensity for the oxymethine group is much lower than that for the protonated aromatic carbons. While the percentages of the fast and slow components had larger errors for the oxymethine group, the fits were generally quite good with high correlation values.

Table 5 shows ^{13}C $T_{1\rho}$ results for an untreated 30/70 blend and 30/70 PS95/PVME99 blends that were treated at 120 and 140 °C for 12 h. The $T_{1\rho}$ values for both the untreated sample and the sample treated at 120 °C are essentially identical within experimental error. When

Table 4. WISE Line Width Results for Heat-Treated 70/30 PS/PVME Blends

	fwhh[a] (kHz) at mixing time (ms) of					
	1	5	10	50	100	200
untreated/126 ppm	29.4	26.1	25.2			
untreated/56 ppm	26.1	22.6	25.7			
heat treatment/peak						
DSC-C2/126 ppm[b]	29.5	27.4	26.5			
DSC-C2/56 ppm[b]	23.0	26.8	28.2			
100 °Cfor 1 week/126 ppm	30.0	27.8	27.0			
100 °C for 1 week/56 ppm	24.8	28.0	26.4			
120 °C for 12 h/126 ppm	29.5	27.3	26.1			
120 °C for 12 h/56 ppm	23.9	25.8	25.4			
140 °C for 12 h/126 ppm	30.8	29.2	28.6		27.9	27.5[c] (27.1)
140 °C for 12 h/56 ppm	18.2	20.6	17.8		22.7	22.6[c] (20.2)

[a] Measured line width at half-height. [b] Sample treated with the same annealing conditions as those in curves 1 and 2 in Figure 4. [c] The experiment was repeated with four times the number of scans.

Table 5. ^{13}C $T_{1\rho}$ Results for Heat-Treated 30/70 PS/PVME Blends

		^{13}C $T_{1\rho}$ (ms)			
		126 ppm		76 ppm	
	peak (%)	long	short	long	short
untreated	46	9.4 ± 0.8	1.17 ± 0.11	1.8 ± 1.1	0.39 ± 0.09
heat treatment at					
120 °C for 12 h	47	8.2 ± 0.6	1.03 ± 0.08	1.0 ± 0.3	0.29 ± 0.12
140 °C for 12 h	80	26.2 ± 0.8	0.90 ± 0.10	10.4 ± 1.3	0.75 ± 0.06

Table 6. ^{13}C $T_{1\rho}$ Results for Heat-Treated 50/50 PS/PVME Blends

		^{13}C $T_{1\rho}$ (ms)			
		126 ppm		76 ppm	
	peak (%)	long	short	long	short
untreated	59	14.9 ± 1.1	0.41 ± 0.03	3.3 ± 0.6	0.34 ± 0.05
heat treatment at					
80 °C for 12 h				4.0 ± 1.0	0.24 ± 0.05
100 °C for 12 h	60	15.5 ± 1.1	1.54 ± 0.18	3.0 ± 1.7	0.58 ± 0.18
120 °C for 12 h	61	13.9 ± 0.7	1.29 ± 0.12	1.9 ± 0.4	0.29 ± 0.07
140 °C for 12 h	78	24.3 ± 1.3	1.24 ± 0.21	8.7 ± 2.4	0.61 ± 0.18
140 °C for 12 h followed by annealing at 100 °C for 24 h	66	16.5 ± 1.3	1.5 ± 0.18	5.2 ± 3.1	0.68 ± 0.23

Table 7. ^{13}C $T_{1\rho}$ Results for Heat-Treated 70/30 PS/PVME Blends

		^{13}C $T_{1\rho}$ (ms)			
		126 ppm		76 ppm	
	peak (%)	long	short	long	short
untreated	75	25.1 ± 1.8	1.71 ± 0.29	10.2 ± 3.4	1.17 ± 0.30
heat treatment					
DSC-C2[a]	77	22.6 ± 1.5	1.30 ± 0.27	6.4 ± 0.8	0.51 ± 0.12
100 °C for 1 week	75	24.0 ± 1.7	1.73 ± 0.32	9.8 ± 1.6	0.95 ± 0.16
120 °C for 12 h	77	24.4 ± 1.5	1.58 ± 0.28	10.5 ± 1.5	0.97 ± 0.13
140 °C for 12 h	78	27.4 ± 1.9	1.34 ± 0.27	8.2 ± 1.4	0.72 ± 0.19

[a] Sample treated with the same annealing conditions as those in curves 1 and 2 in Figure 4.

the sample was treated at 140 °C for 12 h, phase separation occurred, as shown by WISE measurements. Now the components have relaxation behavior similar to pure homopolymers where PS becomes rather rigid and PVME very pliable. Like ^{1}H $T_{1\rho}$'s, ^{13}C $T_{1\rho}$'s will have a minimum when a large proportion of motions have a frequency similar to that of the spin-lock field strength. Additionally, higher or lower frequency motions will result in a larger $T_{1\rho}$ value. As shown in Table 5, there is essentially no difference between ^{13}C $T_{1\rho}$'s and the fraction of the slow $T_{1\rho}$ component in the untreated blend and the blend treated at 120 °C. However, the sample treated at 140 °C exhibits an increase in the $T_{1\rho}$ value, as well as a large increase in the percentage of long $T_{1\rho}$ component.

Table 6 shows ^{13}C $T_{1\rho}$ results for an untreated 50/50 PS95/PVME99 blend as well as samples treated at 80, 100, 120, and 140 °C for 12 h. It is immediately apparent that there is an overall increase in the long $T_{1\rho}$ component for both PS and PVME as compared to the corresponding values for the 30/70 PS95/PVME99 blend. This should be expected since the blend, at temperatures below the LCST, is homogeneous (on a 5 nm scale), and the addition of a more rigid component would increase the rigidity of the whole system. For the blend treated at 140 °C, the long $T_{1\rho}$ and the percentage of that component increase compared to the $T_{1\rho}$'s for the blends preceding it.

Table 7 shows ^{13}C $T_{1\rho}$ results for an untreated 70/30 PS95/PVME99 blend, a 70/30 PS95/PVME99 blend treated in accordance with curves 1 and 2 in Figure 4, a 70/30 PS95/PVME99 blend treated at 100 °C for 1 week, and 70/30 PS95/PVME99 blends treated at 120 and 140 °C for 12 h. Once again there is a substantial

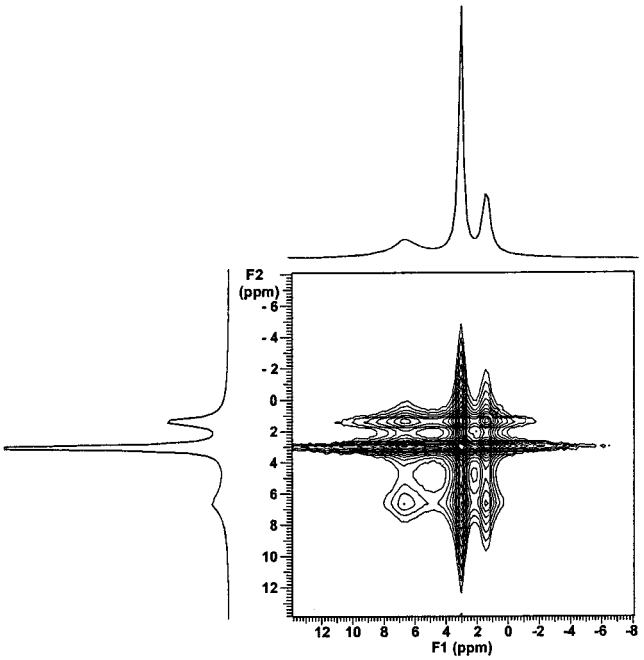

Figure 11. NOESY 2D contour plot of a fresh 50/50 PS/PVME blend at 100 °C.

overall increase in $T_{1\rho}$ for both PS and PVME when compared to both the 30/70 and 50/50 PS95/PVME99 blends, indicating a more rigid sample. Closer inspection of the data reveals that this blend presents a more challenging problem where essentially all the values are equivalent within experimental error. This could suggest that the blend does not phase separate when the sample is treated at 140 °C. However, the WISE data shows nonequilibration of ^{1}H line widths. Furthermore, the sample was transformed from a clear film to completely opaque when treated at 140 °C. These latter observations are ample evidence for phase separation. Therefore, an alternative explanation must be found for the lack of a significant difference in $T_{1\rho}$'s between the samples treated below 140 °C and the sample treated at 140 °C. One possible explanation is that the long $T_{1\rho}$ values for PS at treatment temperatures below 140 °C are already very close to the phase-separated $T_{1\rho}$ value, as can be seen in both the 30/70 and 50/50 PS95/ PVME99 blends. In addition, the long $T_{1\rho}$ value of PVME in the sample treated at 140 °C does not necessarily indicate that it is the same (in a mobility sense) as the values above it. In fact, the long $T_{1\rho}$ value of PVME in the sample treated at 140 °C is to the right of the minimum in the plot of $T_{1\rho}$ vs τ_c rather than on the left like the values preceding it.

^{1}H NOESY Measurements. ^{1}H 2D-NOESY experiments were run on samples at 100 °C rather than heat treating the sample and running the experiment at room temperature. In mobile solutions the NOE is mostly dependent on cross-relaxation. However, in the solid state, spin diffusion can play a role in affecting the intensity of the NOE. Figure 11 shows a representative contour plot of a 2D-NOESY spectrum from a 50/ 50 PS95/PVME99 blend at 100 °C. The experiment shows proton spectra along both the ω_1 and ω_2 dimensions, where the cross-peaks in the contour plot reveal the NOE interactions. Closer examination of the trace along ω_1 shows that the broad downfield resonance is entirely from the aromatic protons of PS. Moreover, the narrow resonance in the middle of the spectrum is only composed of the methoxy and oxymethine protons of PVME. The furthest upfield resonance is composed of the backbone protons of both PS and PVME. Resolution of the component resonances allows the determination of the NOE interaction. The extent of the NOE interaction was determined by comparing the 2D NOESY cross-peak intensities to the peak intensities obtained by a Bloch decay experiment run under similar conditions. Figure 12a shows a 2D NOESY spectrum taken along a slice in the F2 dimension containing the maximum diagonal peak intensity for the methoxy and oxymethine protons of PVME. Figure 12b shows a Bloch decay spectrum acquired with the same experimental parameters as those used to obtain the 2D NOESY spectrum. A 2D slice was also taken along a shift in F2 corresponding to the position containing the maximum diagonal peak intensity for the aromatic protons of PS. The spectrum at this slice was compared with the Bloch decay spectrum. It was found that the PS and PVME cross-peak intensities were 102% and 100%, respectively, relative to the corresponding peaks in the Bloch spectrum. Experimental error was found to be ±8%. Since there is a significant interaction between the PS and PVME protons even at 100 °C, this indicates that phase separation has not occurred. Similar results were found for the 30/70 and 70/30 PS95/PVME99 blends.

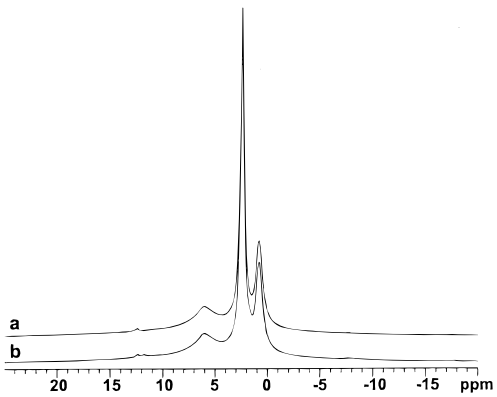

Figure 12. Spectra of a 50/50 PS95/PVME99 blend at 100 °C (a) 2D NOESY slice obtained with a mixing time of 300 ms. (b) Bloch decay spectrum.

Discussion

Figure 13 shows the cloud point (T_b) dependence on composition (hereafter referred to as the binodal curve), determined from laser light scattering. In addition, the composition dependence of glass transition temperatures (T_{gi}, T_{gm}, and T_{gf}) determined from DSC for the PS95/ PVME99 blend is plotted. It should be mentioned that laser light scattering, which was used to determine values of T_b, could not be used to detect domain sizes smaller than approximately 500 nm, whereas solid-state NMR spectroscopy could be used to detect domain sizes on the order of 5 nm in untreated samples at room temperature. If we accept a view that a blend can be considered as miscible if it exhibits a single composition-dependent glass transition temperature, we can conclude that the PS95/PVME99 blends are miscible over the entire composition range (see Figure 2). Note, however, that DSC cannot effectively determine domain sizes on the order of 5 nm. These observations lead us to conclude that microheterogeneity exists in the miscible PS95/PVME99 blends at temperatures below T_b. However, it is clear that the homogeneity of a polymer

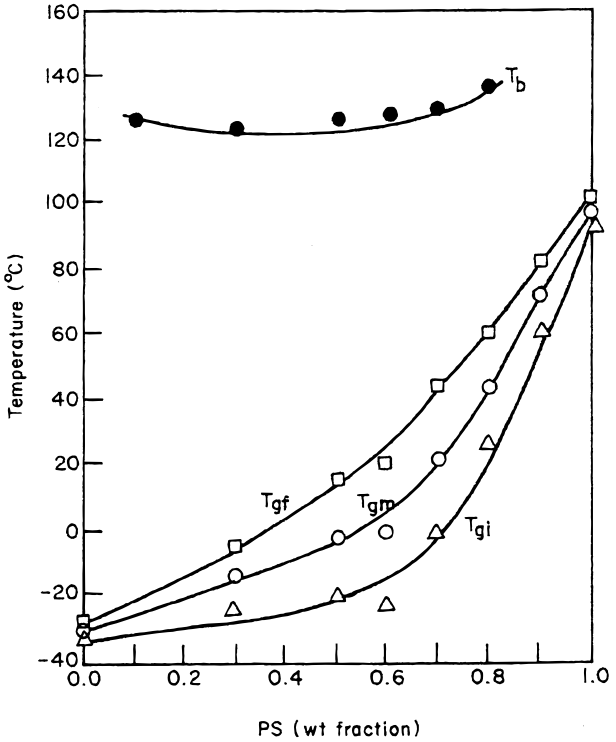

Figure 13. Composition dependence of cloud point determined from light scattering experiment (●) and composition dependence of glass transition temperature: T_{gi} (○), T_{gm} (△), and T_{gf} (□) for the PS95/PVME99 blend system investigated in this study.

blend is dependent on the minimum domain size detectable by the experimental technique used.

^{1}H $T_{1\rho}$ measurements show that PVME affects the segmental motions of PS, and vice versa. At temperatures above 45−80 °C, depending on blend composition, the divergence in ^{1}H $T_{1\rho}$ values was first thought to be an indication that there was an increase in the degree of phase separation of the two components on a molecular level. Li et al.[39] have shown that this may be the case in blends of poly(2,6-dimethylphenylene ether) and PS. However, from T_2 measurements[36] it was found that at temperatures above 45 °C the rate of spin diffusion was such that ^{1}H T_{1p} measurements could only be used to determine domains smaller than about 2 nm. Since domains on the order of 5 nm exist within the untreated blend samples, ^{1}H $T_{1\rho}$ could not be used to determine whether larger domains formed when the temperature was raised. Fortunately, the ^{1}H $T_{1\rho}$ measurements did give valuable information. They show that there is motional heterogeneity within the blends and that each component begins to assume relaxation characteristics similar to their pure homopolymers at high temperatures.

Considering the large difference in mobility observed in Figure 9, let us reexamine the effect of cooling rate on the shape of the DSC traces shown in Figure 4. A 70/30 PS95/PVME99 blend at 100−120 °C has a large difference in component mobility. This probably results in compositional fluctuations. Recently, on the basis of a rheological investigation, Kim et al.[40] concluded that dynamic composition fluctuations exist near the critical point (LCST) of a PS/PVME blend system. The fact that NMR reveals only domains on the order of 5 nm does not mean that larger domains do not exist. Spin diffusion measurements equilibrate to the smallest average domain size. Hence, when this specimen was quenched very rapidly from 100−120 to −40 °C at a rate of 200 °C/min, the component chains in the blend may have been frozen. Under such circumstances, the specimen would not have had sufficient time to undergo a transition from a larger microheterogeneous phase (>15 nm borderline miscibility for DSC) to phases on the order of 5 nm. Thus, it would be very difficult for the 70/30 PS95/PVME99 blend to exhibit a clear-cut glass transition temperature. This may be the reason a very broad glass transition is observed in curves 2, 3, and 5 of Figure 4. Conversely, very slow cooling of the microheterogeneous 70/30 PS95/PVME99 blend from 100 to 120 °C to − 40 °C at a rate of 10 °C/h would have provided sufficient time for the specimen to undergo a transition to the smaller (5 nm) microheterogeneous phase. This may explain why we observe a very distinct T_g in curve 4 of Figure 4. If two straight lines are drawn, one from the left side and another from the right side, tangential to curve 2, 3, or 5 of Figure 4, the breadth of the glass transition, $\Delta T_g = T_{gf} - T_{gi}$, can be obtained. This breadth is much greater than that from curve 4 of Figure 4.

Many studies have been conducted on PS/PVME blends. Some of these studies show the blends to be homogeneous while other show that the blends are heterogeneous. Conflicting results can, for the most part, be explained by the method of study. However, some confusion may have resulted from the complexity of this blend system. While we have shown that our blends initially contain small domains on the order of 5 nm, the blends do not phase separate until the LCST is reached. In addition, even though the blends do not phase separate at temperature below the LCST, the component polymers begin to assume the motional characteristics of their respective homopolymers at temperatures above 45−80 °C (depending on blend composition).

Conclusions

While it has been quite common to use the detection of multiple ^{1}H $T_{1\rho}$ relaxation decays as evidence for spatial heterogeneity, it is important to observe that even a completely amorphous homopolymer can give multiple relaxation decays for its different functional groups. This was clearly seen in the PVME homopolymer. In cases where the observation of multiple ^{1}H $T_{1\rho}$ relaxation decays could be from motional heterogeneity and/or spatial heterogeneity, additional experiments are required. WISE measurements show conclusively that small initial domains on the order of 5 nm exist within all of our untreated blend samples. In addition, these measurements show that our PS/PVME blends do not phase separate until the heat treatment temperature is above the LCST (as determined by cloud point measurements). To eliminate the concerns that the phase-separated domains re-formed when the blends were run at room temperature, NOESY experiments were run at 100 °C. These experiments showed strong NOE interactions between both PS and PVME, demonstrating that the component domains had not phase separated at this temperature.

References and Notes

(1) Molnar, A.; Eisenberg, A. *Macromolecules* **1992**, *25*, 5774.
(2) Stoelting, J.; Karatz, F. E.; MacKnight, W. J. *Polym. Eng. Sci.* **1970**, *10*, 133.

(3) Bank, M.; Leffingwell, J.; Theis, C. *J. Polym. Sci., Part A-2* **1972**, *10*, 1097.
(4) Kwei, T. K.; Nishi, T.; Roberts, R. F. *Macromolecules* **1974**, *7*, 667.
(5) Nishi, T.; Wang, T. T.; Kwei, T. K. *Macromolecules* **1975**, *8*, 227.
(6) Nishi, T.; Kwei, T. K. *Polymer* **1975**, *16*, 285.
(7) Davis, D. D.; Kwei, T. K. *J. Polym. Sci., Part B: Polym. Phys.* **1980**, *18*, 2337.
(8) Halary, J. L.; Ubrich, J. M.; Ninzi, J. M.; Monnerie, L.; Stein, R. S. *Polymer* **1984**, *25*, 956.
(9) Ubrich, J. M.; Ben Cheikh, F.; Halary, J. L.; Monnerie, L.; Bauer, B. J.; Han, C. C. *Macromolecules* **1986**, *19*, 810.
(10) Yang, H.; Shibayama, M.; Stein, R. S.; Shimizu, N.; Hashimoto, T. *Macromolecules* **1986**, *19*, 1667.
(11) Schneider, H. A.; Cantow, H.; Wendland, C.; Leikauf, B. *Makromol. Chem.* **1990**, *191*, 2377.
(12) Schneider, H. A.; Wirbser, J. *New Polym. Mater.* **1990**, *2*, 149.
(13) Müller, G.; Stadler, R.; Schlick, S. *Makromol. Chem., Rapid Commun.* **1992**, *13*, 117.
(14) Okada, M.; Han, C. C. *J. Chem. Phys.* **1986**, *85*, 5317.
(15) Han, C. C.; Okada, M.; Muroga, Y.; McCrackin, F. L.; Bauer, B. J.; Tran-Cong, Q. *Polym. Eng. Sci.* **1986**, *26*, 3.
(16) Shibayama, M.; Yang, H.; Stein, R. S.; Han, C. C. *Macromolecules* **1985**, *18*, 2179.
(17) Han, C. C.; Okada, M.; Muroga, Y.; Bauer, B. J.; Tran-Cong, Q. *Polym. Eng. Sci.* **1986**, *26*, 1208.
(18) Lau, S.; Pathak, J.; Wunderlich, B. *Macromolecules* **1982**, *15*, 1278.
(19) Widmaier, J.; Mignard, G. *Eur. Polym. J.* **1987**, *23*, 989.
(20) Lin, J. L.; Roe, R. J. *Polymer* **1988**, *29*, 1227.
(21) Trask, C. A.; Roland, C. M. *Macromolecules* **1989**, *22*, 256.
(22) Roland, C. M.; Ngai, K. L. *Macromolecules* **1991**, *24*, 2261.
(23) Roovers, J.; Toporwoski, P. M. *Macromolecules* **1992**, *25*, 3454.
(24) Stejskal, E. O.; Memory, J. D. *High-Resolution NMR in the Solid State, Fundamentals of CP/MAS*; Oxford University Press: New York, 1994.
(25) Chu, C. W.; Dickinson, L. C.; Chien, J. W. *J. Appl. Polym. Sci.* **1990**, *41*, 2311.
(26) Schmidt-Rohr, K.; Clauss, J.; Spiess, H. W. *Macromolecules* **1992**, *25*, 3273.
(27) Goldman, M.; Shen, L. *Phys. Rev.* **1966**, *144*, 321.
(28) Kaplan, S. *Polym. Prepr. Am. Chem. Soc., Div. Polym. Chem.* **1984**, *25* (1), 356.
(29) Jack, K. S.; Whittaker, A. K. *Macromolecules* **1997**, *30*, 3560.
(30) Takegoshi, K.; Hikichi, K. *J. Chem. Phys.* **1991**, *94*, 3200.
(31) Bielecki, A.; Burum, D. P. *J. Magn. Reson., Ser. A* **1995**, *116*, 215.
(32) Fyfe, C. A. *Solid State NMR for Chemists*; C.F.C. Press: Guelph, Ontario, Canada, 1983.
(33) McBriety, V. J.; Packer, K. J. *Nuclear Magnetic Resonance in Solid Polymers*; Cambridge University Press: Cambridge, 1993.
(34) Menestrel, C. Le; Kenwright, A. M.; Sergot, P.; Lauprêtre, F.; Monnerie, L. *Macromolecules* **1992**, *25*, 3020.
(35) Asano, A.; Takegoshi, K.; Hikichi, K. *Polymer* **1994**, *35*, 5630.
(36) Wagler, T. A. Doctoral Dissertation, The University of Akron, Akron, OH, 1999.
(37) Polios, I. S.; Soliman, M.; Lee, C.; Gido, S. P.; Schmidt-Rohr, K.; Winter, H. H. *Macromolecules* **1997**, *30*, 4470.
(38) For a range of diffusion coefficients between 0.02 and 2 nm^2/ms the domain size d is calculated to be between 1.2 and 11.2 nm based on the equation $d/4 = (D_{eff} t_m \pi/4)^{1/2}$, where d is the domain size, D_{eff} is the effective diffusion coefficient, and t_m is the mixing time (5 ms).
(39) Li, S.; Dickinson, C.; Chien, J. *J. Appl. Polym. Sci.* **1991**, *43*, 1111.
(40) Kim, J. K.; Lee, H. H.; Son, H. W.; Han, C. D. *Macromolecules* **1998**, *31*, 8566.

MA9909105